Application of hyperspectral remote sensing to cyanobacterial blooms in inland waters

CrossMark

Raphael M. Kudela [a,*], Sherry L. Palacios [b], David C. Austerberry [c], Emma K. Accorsi [d], Liane S. Guild [e], Juan Torres-Perez [f]

[a] Ocean Sciences Department, 1156 High Street, University of California Santa Cruz, Santa Cruz, CA, USA
[b] ORAU/NASA Ames Research Center, M.S. 245-4, Bldg. 245, Rm. 120, PO Box 1, Moffett Field, CA 94035, USA
[c] Department of Atmospheric, Ocean, and Space Sciences, University of Michigan, USA
[d] Applied Math and Computer Science, Emory University, Atlanta, GA, USA
[e] Earth Science Division, NASA Ames Research Center, M.S. 245-4, Bldg. 245, Rm. 120, PO Box 1, Moffett Field, CA 94035, USA
[f] BAERI/NASA Ames Research Center, M.S. 245-4, Bldg. 245, Rm. 120, PO Box 1, Moffett Field, CA 94035, USA

ARTICLE INFO

ABSTRACT

Cyanobacterial blooms are increasingly posing a severe threat to inland waters, particularly at the land-sea interface where toxins can be transported downstream with subsequent impacts to both terrestrial and marine organisms. These blooms are relatively easy to detect optically because of the surface concentration of cells, the presence of phycocyanin pigments, and the elevated backscatter associated with cell size and the presence of gas vacuoles. Major challenges limiting the use of remote sensing have been, first, that many of these water bodies are small relative to the spatial resolution of ocean color satellites, and second, even with a bright algal target, the spectral resolution, signal-to-noise ratio, and repeat time for terrestrial satellites is often inadequate. The next generation of multispectral and hyperspectral sensors begin to address these issues with both increased spatial and spectral resolution. Weekly monitoring of Pinto Lake, California has demonstrated that this small water body provides an ideal testbed for development and application of algorithms applicable for legacy and next-generation sensors. Pinto Lake experiences seasonal nearly monospecific blooms with a pronounced species succession. Biomass (as chlorophyll) within Pinto Lake seasonally ranges from ~1 to 1000 µg/L. Pinto Lake has been within the flight lines for several recent airborne missions, including the HyspIRI Preparatory Flight Campaign, and is often targeted for HICO acquisitions. Using these data we demonstrate that spectral-shape algorithms requiring minimal atmospheric correction can be used across a range of legacy sensors to detect cyanobacterial blooms and that, with the availability of high spectral resolution data and appropriate atmospheric correction, it is possible to separate the cyanobacterial genera *Aphanizomenon* and *Microcystis*. In California *Aphanizomenon* is typically non-toxic and blooms prior to toxin-producing *Microcystis*, thus leading to the potential for an early warning system based on the identification of algal types.

1. Introduction

In California, there is increasing evidence that freshwater cyanobacteria (blue-green algae) are a growing problem in lakes and rivers. *Microcystis aeruginosa* in particular is considered a cyanobacterial harmful algal bloom (CyanoHAB) organism because it can impede recreational use of waterbodies, reduce esthetics, lower dissolved oxygen concentration, and cause taste and odor problems in drinking water,

as well as produce microcystins, powerful hepatotoxins associated with liver cancer and tumors in humans and wildlife (Carmichael, 2001). Extensive *Microcystis* blooms with toxin production occur during summer and fall in impaired waterways in Washington, Oregon and California (Gilroy, Kauffman, & Hall, 2000; Johnston & Jacoby, 2003) and *Microcystis* contamination has been documented at the marine outflows of the Klamath and San Francisco estuaries (Fetcho, 2007; Lehman, Boyer, Hall, Waller, & Gerhrts, 2005) as well as from river inputs to Monterey Bay (Gibble & Kudela, 2014; Miller et al., 2010). The direct impact to the threatened California Sea Otter (*Enhydra lutris*) has promoted these blooms and toxins from predominantly a freshwater issue to potentially a land–sea problem, with concomitant risk because of the lack of monitoring in brackish and marine waters (Miller et al., 2010). Other common bloom-forming pelagic cyanobacteria

* Corresponding author. Tel.: + 1 831 459 3290.
E-mail addresses: kudela@ucsc.edu (R.M. Kudela), sherry.l.palacios@nasa.gov (S.L. Palacios), dauster@umich.edu (D.C. Austerberry), emma.accorsi@gmail.com (E.K. Accorsi), liane.s.guild@nasa.gov (L.S. Guild), juan.l.torresperez@nasa.gov (J. Torres-Perez).

include *Aphanizomenon, Anabaena*, and (less common, but present, in California) *Lyngbya* (Kurobe et al., 2013); however, since toxicity is primarily associated with *Microcystis*, these other CyanoHABs are generally considered nuisance blooms rather than acutely dangerous to humans and wildlife (Backer et al., 2010; Kudela, 2011; Lehman, Marr, Boyer, Acuna, & Teh, 2013).

Both toxigenic (capable of producing toxin) and non-toxic strains of *Microcystis* are present in California (Baxa, Kurobe, Ger, Lehman, & The, 2010; Lehman et al., 2013; Moisander, Lehman, Ochiai, & Corum, 2009). *M. aeruginosa* bloom formation and consequent toxin generation is influenced by environmental variables such as high nutrient supply, elevated light levels, and warm temperatures (Davis, Berry, Boyer, & Gobler, 2009; Jacoby, Collier, Welch, Hardy, & Crayton, 2000; Paerl & Huisman, 2008; Paerl & Otten, 2013; Tsuji et al., 1994; Welker & Steinburg, 2000; Zehnder & Gorham, 1960). The prevalence of CyanoHABs and subsequent toxic events may be intensified by a warming climate in tandem with increases in environmental degradation and eutrophication (Davis et al., 2009; Guo, 2007; Kudela, 2011; O'Neil, Davis, Burford, & Gobler, 2012; Paerl & Huisman, 2008; Welker & Steinburg, 2000; Zehnder & Gorham, 1960).

While toxin events are primarily associated with *M. aeruginosa*, other potentially toxic genera, including *Aphanizomenon, Anabaena*, and *Planktothrix* are frequently present in impacted water bodies (Kudela, 2011). These genera often produce dense surface blooms (Lehman et al., 2013; Paerl, 2008; Sellner, 1997), making satellite detection of potentially harmful cyanobacterial blooms possible (e.g. Kahru, 1997; Simis, Peters, & Gons, 2005, Simis et al., 2007; Vincent et al., 2004; Wynne et al., 2008). One issue with these methods is that not all cyanobacterial genera are toxic, nor is toxin always produced by toxigenic species. Thus while it is possible to identify potential CyanoHABs, it is desirable to separate potentially toxic and non-toxic blooms.

Many of the optical detection methods for identification of cyanobacterial blooms rely on algorithms targeting phycocyanin (reviewed by Kutser, 2009 and Ogashawara, Misra, Mishra, Curtarelli, & Stech, 2013), a characteristic pigment associated with freshwater cyanobacteria. Phycocyanin is a pigment-protein complex with a broad absorption feature at ~620 nm, often detected from remote sensing data using a wavelength range of 615–630 nm (Ogashawara et al., 2013). Potential issues with these approaches include the necessity to acquire data at sufficiently fine enough spatial and spectral resolution to identify the phycocyanin absorption feature in remote sensed data, the sensitivity to poor remote sensing data due to (for example) inadequate atmospheric correction (Wynne, Stumpf, Tomlinson, & Dyble, 2010), and the lack of a "universal" algorithm applicable to all sensors (Kutser, 2009).

One approach that avoids issues with atmospheric correction and is more easily extensible to multiple sensors involves the use of spectral shape, rather than identification of specific absorption features. In particular, Wynne et al. (2008, 2010) demonstrated that spectral shape (or the second derivative of the remote sensing reflectance spectrum) is insensitive to atmospheric correction when applied to surface-intensified blooms of cyanobacteria. Those authors developed a Cyanobacterial Index (CI) that relies on changes in the shape between 665, 681, and 709 nm caused by the strong scattering by cyanobacteria at around 709 nm (c.f. Wynne et al., 2008). The CI has been successfully applied to the detection of blooms in the Laurentian Great Lakes using the Medium Resolution Imaging Spectrometer (MERIS; Wynne et al., 2008), and later in conjunction with other environmental data such as wind speed (Wynne et al., 2010). A similar spectral shape approach was taken by Matthews, Bernard, and Robertson (2012). Those authors developed the Maximum Peak Height (MPH) algorithm and applied MPH to inland and coastal waters in South Africa with MERIS data. More recently, another generalization of spectral shape algorithms resulted in the Adaptive Reflectance Peak Height (ARPH) algorithm, applied to coastal waters of Monterey Bay, California, using the Hyperspectral

Imager for the Coastal Ocean (HICO) by Ryan, Davis, Tufillaro, Kudela, and Gao (2014). All of these algorithms employ spectral shape and demonstrate reduced sensitivity to noisy data, such that they can even be applied to top-of-atmosphere radiances, a method pioneered by Gower, Doerffer, and Borstad (1999) in the development of the Maximum Chlorophyll Index (MCI) for MERIS.

Despite advances in development of both semi-analytical phycocyanin methods and spectral shape methods (Ogashawara et al., 2013), remote-sensing methods for detection of cyanobacterial HABs are still limited by the relative unavailability of sensors with both fine spectral and spatial resolution. Planned sensors such as the European Space Agency's Ocean Land Color Instrument (OLCI) aboard Sentinel-3 and NASA's Hyperspectral Infrared Imager (HyspIRI) will provide both greatly improved spectral and spatial resolution, but are not yet available. This limitation has hindered the application of remote sensing for routine monitoring and detection of CyanoHABs in California, despite widespread interest by monitoring and management agencies. To address these issues, and in preparation for the routine availability of data products from OLCI, HyspIRI, and other sensors, we took advantage of airborne data from the NASA Student Airborne Research Program (SARP, 2009 and 2011) and the HyspIRI Airborne Campaign (2013) collected over central California. Flights routinely imaged Pinto Lake, a small, hyper-trophic water body located adjacent to Monterey Bay, California. Pinto Lake is well characterized in terms of CyanoHAB events (Kudela, 2011) and makes an ideal testbed for development and testing of remote sensing algorithms. As with other inland waters, Pinto Lake also exhibits a regular successional pattern with increases in the (generally non-toxic) organism *Aphanizomenon* preceding blooms of the highly toxic *Microcystis aeruginosa*. Here we demonstrate that a two-step approach, first identifying the presence of potential CyanoHABs, and second, separating *Aphanizomenon* from *Microcystis*, may provide an early-warning capability for detection of potentially harmful blooms.

2. Materials and methods

2.1. Study area and sampling strategy

The primary study area was Pinto Lake, California (36.95° N, 121.77° W). Pinto Lake is a shallow natural lake located 8.3 km inland from Monterey Bay (Fig. 1). This spring-fed lake has a maximum depth of ~10 m and covers 37 surface hectares. Pinto Lake includes parks operated by the City of Watsonville and Santa Cruz County, and is regularly used for recreational activities including fishing and boating. Two other water bodies were used as qualitative validation for the algorithm development. Kelly Lake is immediately adjacent to Pinto Lake (36.94° N, 121.74° W). It covers 36 surface hectares and has a maximum depth of ~6 m. There is no public access, which precluded routine monitoring. A third water body, Campus Lagoon at the University of California Santa Barbara (34.40° N, 119.84° W) was also sampled opportunistically as part of the field effort.

Of the three study areas, Kelly Lake and Campus Lagoon were sampled a single time, and were included as verification sites for the algorithms, which were developed with the more extensive data available from Pinto Lake. The latter has been sampled approximately weekly since August 2009. Data include relative cell abundance determined by microscopy, surface chlorophyll concentration, temperature, and toxin as both whole-water "grab" samples and integrated toxin using the Solid Phase Adsorption Toxin Tracking (SPATT) methodology. While microcystins include more than 90 chemical congeners, the most common and routinely reported form is microcystin LR (MCY-LR); we therefore used the concentration of MCY-LR (ppb) in this analysis. Details of the time-series are provided in Kudela (2011). For part of the time series phycocyanin was measured by fluorescence using an Algae Torch (BBE). The fluorescence was converted to equivalent μg/L concentration using discrete samples that were extracted and analyzed
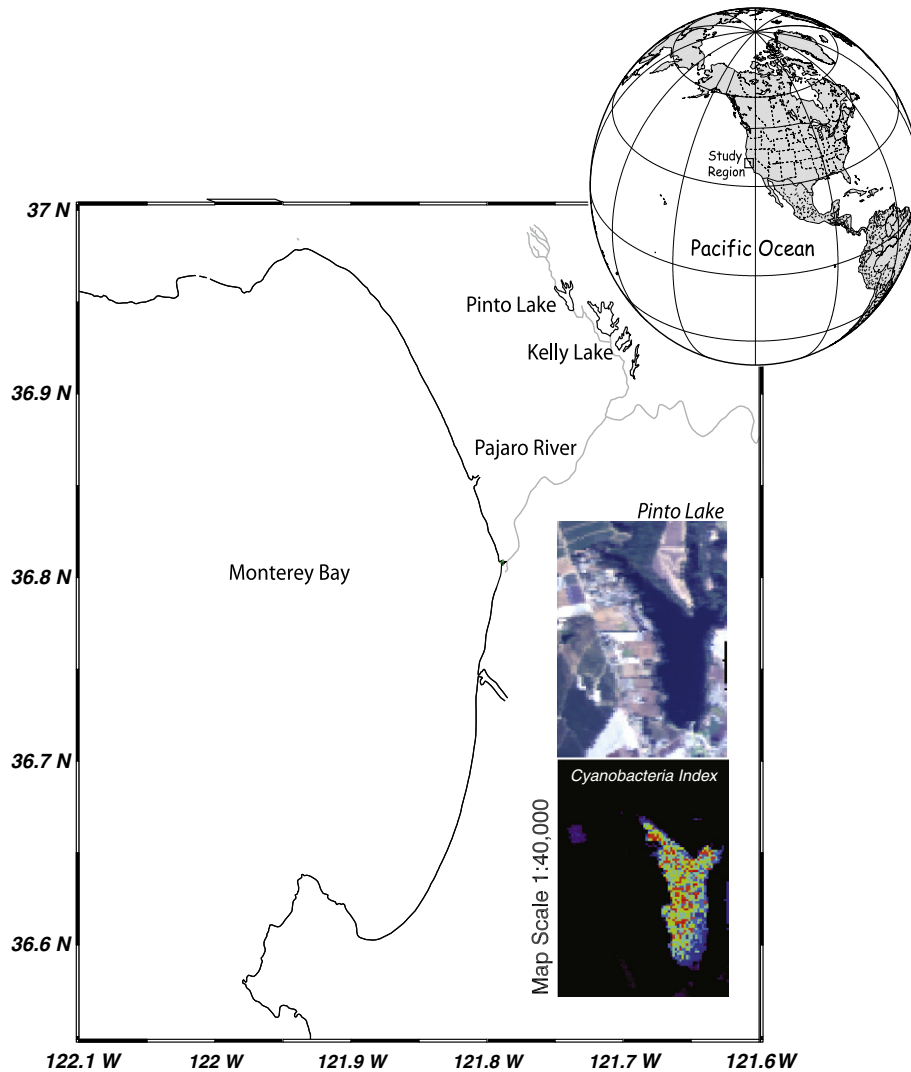
Fig. 1. The geographical location of the primary study site, containing Pinto Lake, and Kelly Lake. The greater Monterey Bay, California region is one of the HyspIRI Airborne Campaign regional targets. The inset images provide AVIRIS imagery for 31 October 2013 depicting true-color (top) and the CI (bottom). Sampling occurred at the boat dock, visible in the bottom middle part of the true-color image.

by spectrometer (Sampath-Wiley & Neefus, 2007). Other data reported herein were collected as described by Kudela (2011). As described therein, phytoplankton taxa were enumerated on a relative abundance index and reported as not present, rare, common, abundant, or dominant, based on visual examination by microscopy using a Leica MZ12 microscope.

2.2. Field optical data

Remote sensing reflectance ($R_{rs}(\lambda)$), defined as the upwelling radiance emerging from the water body divided by the incident downwelling irradiance, was determined at Pinto Lake using either a PANalytical (formerly Analytical Spectral Devices, Boulder, CO) FieldSpec spectroradiometer equipped with a 7.5° foreoptic, or a Spectra Vista (Poughkeepsie, NY) GER 1500, both for the selected wavelength range of 400–800 nm. Radiance data were collected and processed following the methods described in Lee et al. (1997), with multiple spectra acquired and averaged for each time point. Spectra were normalized using a Spectralon (Labsphere, NH) white (98% albedo) plaque. Spectra corresponding to periods dominated by *Aphanizomenon*, *Microcystis*, mixed assemblages, and non-CyanoHAB organisms were collected during 2012–2013. For

convenience the wavelength notation is omitted from R_{rs} for the remainder of the manuscript.

To complement the above-water R_{rs} data, absorption, scattering, and backscattering data were acquired on 10 July 2012 and 26 July 2012, periods when *Microcystis* (former) and *Aphanizomenon* (latter) dominated. Surface water was collected and transported to the laboratory, where it was pumped through a WETLabs ac-s spectrometer, then filtered and re-measured to provide total (absorption, a m^{-1}, attenuation, c m^{-1}) and dissolved spectra. A HOBI Labs HS-6 was deployed in the near surface (coincident with the FieldSpec measurements) to provide backscatter at six wavelengths. Discrete samples were also collected for particulate (filter-pad) absorption, colored dissolved organic material (CDOM) absorption, and chlorophyll following the methods described in Kudela, Garfield, and Bruland (2006). Whatman GF/F filter (nominally 0.7 μm) were used for pigments and filterpad absorption measurements. *Microcystis* and *Aphanizomenon* are both colonial, with individual spherical cells 2–3 μm in diameter (*Microcystis*) and cylindrical cells ~5 × 100 μm (*Aphanizomenon*). Individual cells are rarely observed, while colonies can be millimeters in diameter, often forming dense surface mats or scums under bloom conditions.

Field data were generally collected from a single location or a small range of locations at the southern end of Pinto Lake (Fig. 1). In contrast, the spatial resolution of the airborne and satellite imagery results in

spatial averaging over a much larger region (tens to hundreds of meters). This mismatch is somewhat mitigated by the small size of Pinto Lake; during blooms, the water was generally homogenous over hundreds of meters, based on discrete samples collected at multiple sites including the boat dock, lake shore, and earthen berms extending into the lake (for example 13 September 2012, Table 1, where all parameters from multiple sites were available and were included in the analysis). However, field sampling was not comprehensive and we did not fully characterize spatial homogeneity across the lake, which does introduce pixel-to-pixel variability in the remote sensing imagery.

2.3. Remote sensing data

Radiometric data were collected using the MODIS/ASTER Airborne Simulator (MASTER). MASTER is an airborne sensor with fine spatial resolution (10–60 m, depending on flight elevation) but limited spectral bands (Table 2). MASTER data were acquired as part of SARP on 22 July 2009 and 30 June 2011 with a ground sample resolution (GSR) of ~20 m. MASTER data were collected as part of the HyspIRI Airborne Campaign on 10 April 2013 and 31 October 2013 at 50 m GSR. Data were atmospherically corrected using the Fast Line-of-sight Atmospheric Analysis of Hypercubes (FLAASH) module provided as part of ENVI (Exelis, Boulder, CO). Imagery from the Hyperspectral Imager for the Coastal Ocean (HICO; Table 2) were obtained from Oregon State University as L2 (atmospherically corrected, 100 m GSR at nadir) using the beta processing software implementation of Tafkaa (Gao, Montes, Ahmad, & Davis, 2000) provided by Oregon State University. No optimization was performed; Tafkaa runs were carried out using an aerosol optical depth (550 nm) of 0.1, and an ozone value of 0.270 ppm.

2.4. Hydrolight simulations

Remote sensing reflectance spectra (R_{rs}; sr^{-1}) were simulated using the Hydrolight 4.0 (Sequoia Scientific) radiative transfer model (Mobley, 1995) to calculate end-member reflectance for *Aphanizomenon* and *Microcystis* blooms, and to explore algorithm sensitivity to inherent optical properties. User-supplied absorption (a, m^{-1}) and attenuation (c, m^{-1}) were obtained from the ac-s data.

Table 1
A summary of the environmental conditions associated with each sampling event depicted in Figs. 3 and 5 for Pinto Lake, CA. The numbers/letters following the date indicate the spectra annotations in Fig. 5.

Date	Chlorophyll a (μg/L)	Phycocyanin (μg/L)	Microcystin LR (ppb)
Above-water spectra			
2-Jun-12 (1)	437.06	74.70	0.63
10-Jul-12 (2)	18.00	38.70	0.33
26-Jul-12 (3)	92.20	38.30	64.31
29-Jul-12 (4)	350.70	43.10	1.81
5-Aug-12 (5)	252.00	30.40	5.54
13-Sep-12 (6)	56.46	29.50	0.00
13-Sep-12 (6)	42.44	35.50	0.00
13-Sep-12 (6)	53.19	40.70	0.00
17-Oct-12 (7)	2253.07	156.70	48.85
3-Apr-13 (8)	118.07	60.30	0.00
10-Apr-13 (9)	72.33	44.40	0.00
31-Oct-13 (10)	94.08	48.90	1.20
5-Dec-13 (11)	10.58	12.80	11.74
HICO			
17-Nov-10 (a)	726.60	28.10	10.28
3-May-11 (b)	23.39	0.00	0.10
12-Sep-11 (c)	108.27	86.80	2.56
26-Oct-11 (d)	474.60	162.90	19.31
9-Nov-11 (e)	680.00	261.50	6.43
15-Jun-12 (f)	8.65	12.10	0.10
20-Aug-12 (g)	22.81	3.70	0.64
27-Aug-12 (h)	27.71	5.90	0.10
6-Nov-12 (i)	2609.25	38.70	4.00

A pure-water phase function was chosen, with fluorescence from chlorophyll and CDOM, and Raman scattering. CDOM absorption was set to a constant value of 0.1 m^{-1} with an exponential decay function and gamma value of 0.014, while chlorophyll absorption was wavelength-specific, using Morel (1998). Model wavelengths from 400 to 785 nm (10 nm intervals) was chosen with infinite depth at 0.5 m steps to 1.5 m. Sky conditions were set to a solar zenith-angle of 10°, 0% cloud cover, no wind, and default sky conditions based on RADTRAN. While the modeled solar zenith angle is not typical for HICO (which is typically ~45°), the Hydrolight runs were used primarily to test the sensitivity to changes in chlorophyll concentration and backscatter ratio. An array of model runs was performed, varying the backscatter ratio from 0.001 to 0.0150 and varying chlorophyll from 5 to 20 mg m^{-3}.

2.5. Algorithm development

We employed a suite of algorithms for characterization of cyanobacterial biomass and separation of *Aphanizomenon* and *Microcystis* from remote sensing reflectance data. These included the Cyanobacteria Index, CI (Wynne et al., 2008, 2010), and several empirically-derived spectral shape algorithms derived from observed data and Hydrolight runs. These algorithms were applied to MASTER and HICO data to assess applicability and are provided in Table 3 and Fig. 2. Following the convention of Wynne et al. (2008, 2010) we define a spectral shape algorithm using MASTER bands 654 nm, 714 nm, and 754 nm to estimate the Scattering Line Height (SLH), and a set of spectral shape algorithms for distinguishing *Aphanizomenon* versus *Microcystis* as the *Aphanizomenon-Microcystis* Index (AMI) as described in Table 3.

The AMI was developed by empirical comparison of various spectral shape parameters using known spectra from field samples. Samples varied from nearly 100% *Microcystis* to nearly 100% *Aphanizomenon*. For the AMI, spectra were first normalized by setting the maximum peak height between 700 and 720 nm to unity. CI and SLH were applied without normalization of the R_{rs} spectra. There was no *a priori* reason for selecting the subset of bands and spectral shapes used, although selection was guided by documented optical characteristics such as the known influence of phycocyanin absorption and cell scattering (e.g. Ogashawara et al., 2013; Wynne et al., 2008). In the development of SLH and AMI, other possible band and spectral shape combinations were tested by comparing results to Hydrolight and above-water spectra. The final (AMI, SLH) algorithms were chosen based on comparison to field data by maximizing the r^2 value between the indices and measured properties (phycocyanin, relative abundance of cyanobacterial genera) using linear regression.

3. Results

3.1. Environmental overview of field sites

Pinto Lake, California exhibits strong seasonality in ecological and bio-optical properties (Kudela, 2011; Table 1; Fig. 3). This hyper-eutrophic lake frequently exhibits toxin concentrations vastly exceeding California Office of Environmental Health Hazard Assessment (OEHHA) recommended alert levels of 0.8 ppb total microcystin (Butler, Carlisle, & Linville, 2012). Similar to other systems (Lehman, McDonald, & Lehman, 2009; McDonald & Lehman, 2013), dominance by *Aphanizomenon spp.* generally preceded *Microcystis aeruginosa*, presumably due to a combination of water chemistry (*Aphanizomenon* is capable of fixing atmospheric nitrogen, while *Microcystis* does not possess this capability; Lehman et al., 2009) and temperature (Paerl, Hall, & Calandrino, 2011). Within Pinto Lake, toxin-production is also associated with *Microcystis*, while blooms of cyanobacteria including *Anabaena spp.* and *Aphanizomenon flos-aquae* are not associated with production of microcystins (Kudela, 2011). Relevant to this study, microcystins were detected in both Kelly Lake and the UCSB Lagoon during

Table 2
Characteristics of current and future sensors relevant to studies of inland waters.

Sensor	Wavelength	Bands	IFOV	Swath width	GSR	Reference
MASTER	0.4–13.0 μm	50	2.5 mrad	14.3 km (DC-8) 35.8 km (ER-2)	20 m (DC-8) 50 m (ER-2)	Hook, Myers, Thome, Fitzgerald, & Kahle (2001)
HICO	0.35–1.07 μm[a]	128	0.238 mrad	42 km[b]	83 m[b]	Lucke, Corson, McGlothlin, Butcher, & Wood (2010)
HyspIRI	0.38–2.5 μm	2462	–	145 km	60/1000 m	Devred et al. (2013)
OLCI	0.4–1.02 μm	21	–	1270 km	300/1200 m	IOCCG (2014)
PACE[c]	0.35–0.8 nm	90	–	–	1000 m	PACE (2012)

[a] Useful range is 400–800 nm.
[b] Nadir resolution.
[c] Threshold requirements.

opportunistic sampling conducted as part of field validation of the remote sensing data.

3.2. Development of the Scattering Line Height (SLH) index

Hydrolight runs simulating remote sensing reflectance for *Microcystis* demonstrate that a spectral shape algorithm centered on the MASTER band at 714 nm is indicative of the presence of cyanobacteria. As expected from studies of chlorophyll fluorescence and scattering (i.e. Gower et al., 1999), the reflectance spectra show that the chlorophyll fluorescence peak increases in amplitude and shifts slightly to longer wavelengths as the backscatter ratio increases. However, a comparison of spectra for different chlorophyll concentrations shows that while the amplitude of the fluorescence peak increases with chlorophyll concentration, the reflectance at the peak's red shoulder does not change appreciably (Fig. 4). The SLH algorithm takes advantage of this property to estimate the probability of surface-forming blooms of cyanobacteria.

Remote sensing reflectance (Fig. 5) was calculated for Pinto Lake using both HICO and above-water reflectance measurements. The HICO data clearly exhibit issues with atmospheric correction (e.g. negative reflectances in the blue part of the spectrum) and reduced spectral resolution compared to the above-water measurements, but consistent spectral shapes are evident in both datasets. Here we deliberately use both datasets to demonstrate that spectral shape algorithms are reasonably robust to bad data.

Fig. 6 compares the well-described CI algorithm and our SLH algorithm using these data. For HICO, the relationship between phycocyanin concentration and CI is weak ($r^2 = 0.24$, $p = 0.10$) while SLH is much more robust ($r^2 = 0.54$, $p = 0.01$) suggesting that, for potentially noisy data (e.g. HICO), SLH provides a reasonable alternative to CI, making it possible to extend cyanobacterial bloom mapping to sensors that do have bands appropriate for CI. Inclusion of the above-water data does not significantly improve the fit for CI ($r^2 = 0.14$, $p = 0.11$) and results in a decrease for SLH ($r^2 = 0.40$, $p = 0.05$), primarily due to the added variability at low phycocyanin concentrations.

3.3. Separation of Aphanizomenon and Microcystis

In California, *Aphanizomenon* is generally non-toxic, although it has been reported to produce saxitoxins and cylindrospermopsins in other

Table 3
Algorithms developed and/or applied to the spectral data from California inland water bodies. For the AMI, nominal wavelengths from Fig. 2 are provided; the actual wavelengths used are chosen to correspond to the peak (dip) wavelengths of the spectra. *SS* is spectral shape.

Algorithm	Formulation
CI	$CI = -SS(681)$
	$SS(681) = Rrs_{681} - Rrs_{665} - [Rrs_{709} - Rrs_{665}] \times \frac{(681 \text{ nm} - 665 \text{ nm})}{(709 \text{ nm} - 665 \text{ nm})}$
SLH	$SLH = Rrs_{714} - [Rrs_{654} + \frac{Rrs_{754} - Rrs_{654}}{754nm - 654nm}(714 \text{ nm} - 654 \text{ nm})]$
AMI	$AMI = \text{peak width/dip width} = [640 - 510 \text{ nm}] / [652 - 625 \text{ nm}]$

locations (O'Neil et al., 2012). As noted above (see also Fig. 3), *Aphanizomenon* regularly blooms prior to formation of toxic *Microcystis* events in Pinto Lake. This occurred in 2010, 2011, 2012. Dominance by *Aphanizomenon* is usually followed by an overlapping (mixed) community assemblage with *Microcystis*. The phytoplankton assemblage then typically becomes dominated by *Microcystis* and toxin levels increase as the blooms progress (2010–2012), although in 2013, *Microcystis* failed to dominate (Fig. 3) and did not result in the the classic surface-scum blooms that are characteristic of this organism. Temporal separation between *Aphanizomenon* and *Microcystis* is variable, ranging from very short or as in 2013 a prolonged (months) mixture of both organisms with no clear dominance by either genus.

Based on empirical observations and Hydrolight simulations, these two cyanobacterial genera exhibit subtle differences in R_{rs} (Fig. 2). Specifically, blooms dominated by *Microcystis* have a stronger phycocyanin absorption feature, which when coupled with the chlorophyll *a* absorption feature at ~680 nm results in a more pronounced peak in R_{rs} at approximately 655 nm (Fig. 2). This is readily apparent in above-water spectra, and is sufficiently robust that it can be identified from the much coarser HICO data, even with non-optimized atmospheric correction. Taking advantage of this change in spectral shape, the AMI uses the width of the dominant reflectance peak (~565 nm) and the width of the dip caused by phycocyanin absorption (~620 nm) to define a gradient
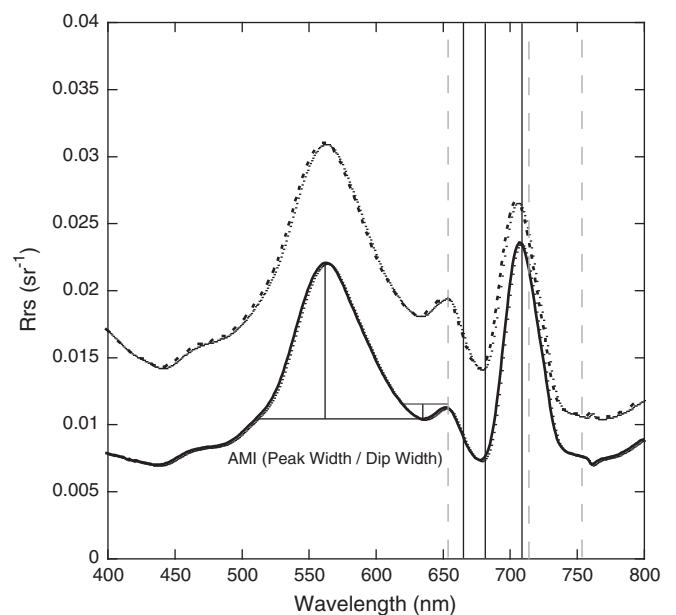

Fig. 2. Example spectra for blooms of *Microcystis* (solid) and *Aphanizomenon* (dashed) from Pinto Lake, CA collected on 13 September and 10 July 2012, respectively. Vertical solid lines indicate the wavelengths used for the CI, vertical dashed lines indicate wavelengths used for SLH. The AMI is based on the ratio of the peak width at ~565 nm and peak trough at ~620 nm.
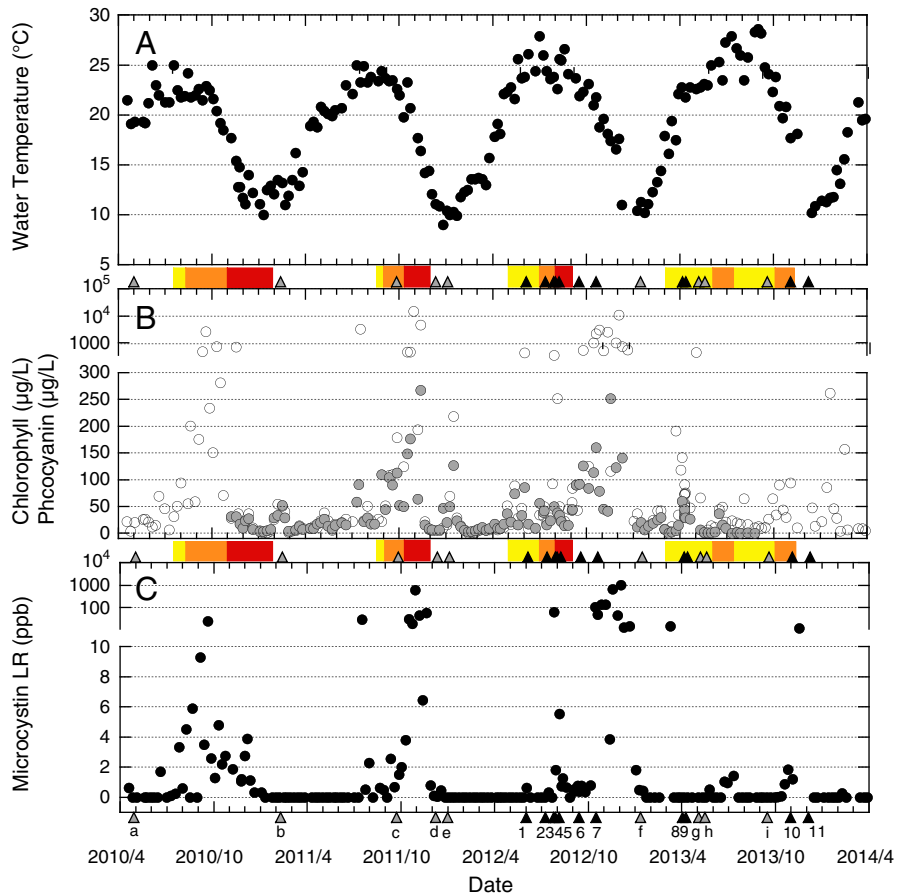
Fig. 3. Time series of approximately weekly water samples collected at Pinto Lake, CA showing (A) water temperature, (B) chlorophyll (open circles) and phycocyanin (shaded circles) concentration, and (C) microcystin LR concentrations. The yellow, orange, and red shading on the timeline denotes periods of dominance by *Aphanizomenon*, a mixed community, and dominance by *Microcystis*, respectively. Black/gray triangles indicate data collection for above-water spectra (black) and HICO imagery (gray). The numbers/letters with the triangles in the bottom panel indicate annotations for the corresponding spectra in Fig. 5.

from *Microcystis* to *Aphanizomenon*. Low AMI values (~2) were empirically determined to be dominated by *Microcystis* while high values (~5) were dominated by *Aphanizomenon*. A caveat of this approach is that the AMI doesn't provide useful information if there is no cyanobacterial bloom.

3.4. Field application of indices

Fig. 7 shows the two biomass indices, the CI and SLH, plotted versus the corresponding microcystin concentration from the same dates for Pinto Lake, and the AMI plotted versus microcystin concentration for
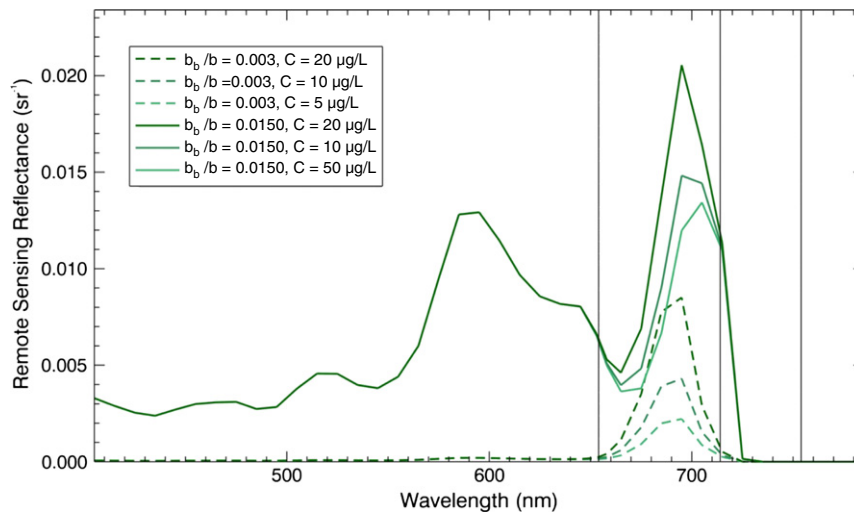

Fig. 4. Results from the SLH algorithm derived from Hydrolight simulations of cyanobacteria, with varying concentrations of chlorophyll and backscattering ratios. SLH is relatively insensitive to changes in chlorophyll. Vertical gray lines indicate MASTER bands used for SLH.
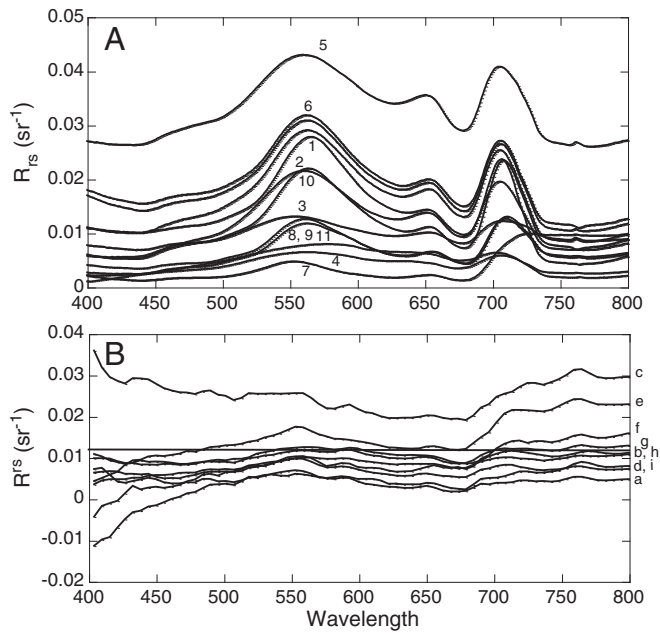
Fig. 5. Remote sensing reflectance for above-water measurements collected using the ASD and GER 1500 (A) and from HICO L2 data (B). Dates are indicated in Fig. 3, and spectra are annotated in Fig. 3 and Table 1. Note the occasional negative reflectances in the HICO spectra.

those dates. The data cluster into several groupings, including high toxicity but low CI or SLH, low toxicity and high CI or SLH, and the "ideal" cluster of increasing CI (SLH) and increasing toxicity. There is a general increase in toxicity with decreasing AMI (increasing dominance by *Microcystis*).

As a demonstration of opportunistic data collection, the SLH algorithm was applied to MASTER data collected in 2009 over Pinto Lake and Kelly
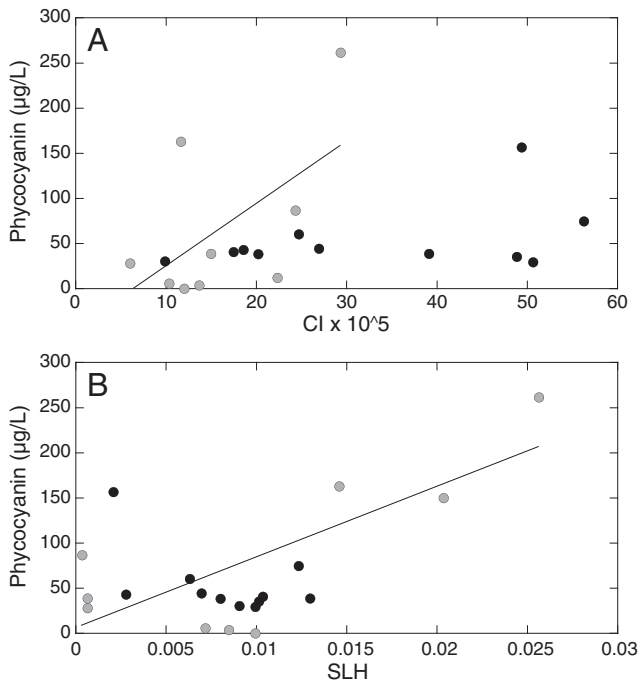

Fig. 6. Scatterplots of phycocyanin from Pinto Lake, CA collected coincident with R_{rs} data used to calculate CI multiplied by 10^4 (A) or SLH (B). Black symbols indicate above-water measurements, gray symbols indicate HICO retrievals. For HICO, the closest water (non-mixed) pixel to the Pinto Lake boat dock was used.
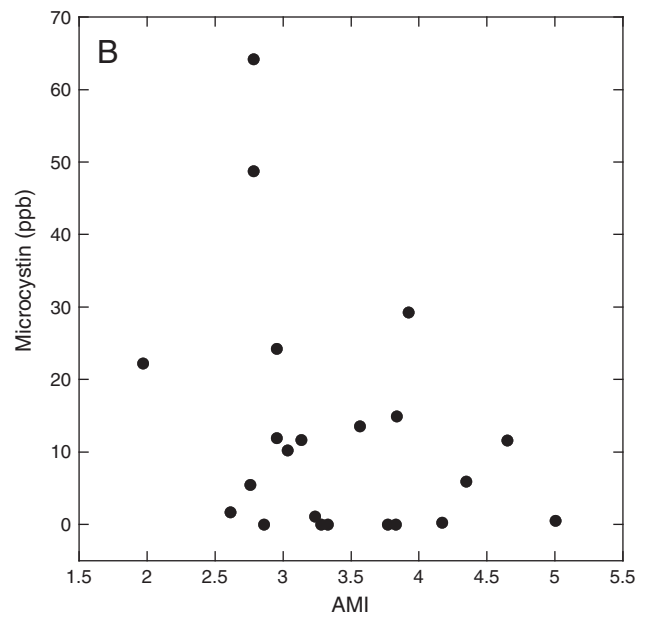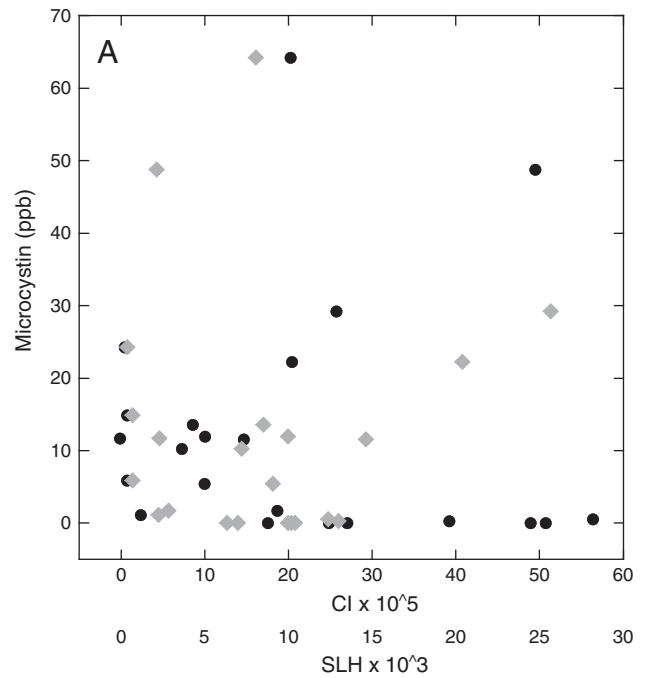

Fig. 7. Scatterplot showing (A) microcystin concentration versus CI (×10^5; solid circles) and SLH (×10^3; gray diamonds) and (B) microcystin concentration versus AMI. Low AMI indicates dominance by *Microcystis*, high AMI indicates dominance by *Aphanizomenon*; intermediate values indicate a mixed assemblage of toxigenic and non-toxic organisms. Increased probability of toxic blooms is indicated by increasing CI or SLH and decreasing AMI values. Note that it is possible to have blooms of non-toxic *Microcystis* and for toxin to be present with low concentrations of *Microcystis*, since toxin concentration is influenced by both the toxicity of the species or strain and the abundance (biomass) of those organisms.

Lake, and in 2011 over the UCSB Lagoon (Fig. 8). A gradient of SLH values were obtained with moderately high values (>0.004 sr⁻¹) for parts of each water body. In each case, verification water samples collected within a few days of the imagery identified the presence of both *Microcystis* and low levels (~0.5 ppb) of microcystin. A similar analysis was applied to Kelly Lake using the HICO image for 26 October 2012. The CI, SLH, and AMI metrics all indicated that Kelly Lake was likely experiencing a bloom of similar composition as Pinto Lake (data not shown). Subsequent water sample verification of that site
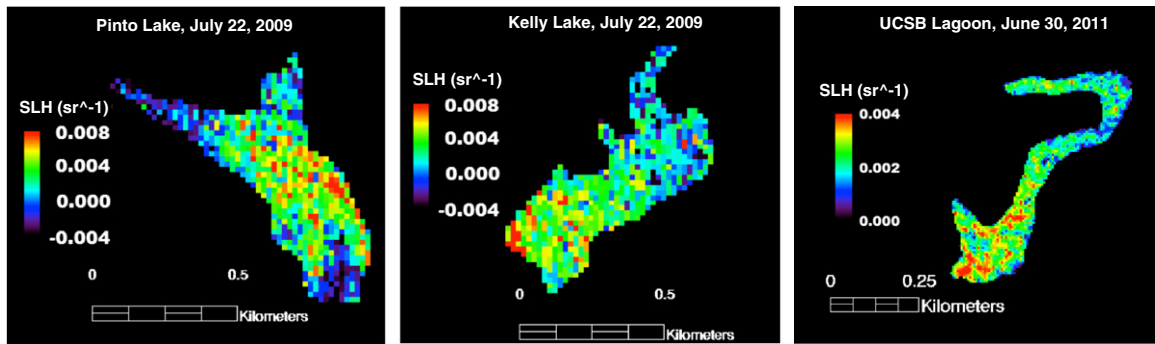
Fig. 8. MASTER data was used to calculate SLH for Pinto Lake, Kelly Lake, and UCSB Lagoon. Warm colors indicate the probability of a cyanobacterial bloom, and were validated with in situ observations.

again confirmed the presence of a cyanobacterial bloom dominated by *Aphanizomenon* with *Microcystis* present.

4. Discussion

While Pinto Lake is a known "hotspot" for CyanoHABs (Kudela, 2011; Miller, Kudela, & Jessup, 2010, 2012, Miller et al., 2010), blooms of potentially toxic cyanobacteria are not well monitored in other California water bodies, other than the San Francisco Bay/Delta (Lehman, Boyer, Satchwell, & Waller, 2008, Lehman et al., 2013), the Klamath River and its reservoirs (c.f. Butler, Carlisle, Linville, & Washburn, 2009; Fetcho, 2007), and Clear Lake (Kurobe et al., 2013). Recent monitoring results suggest that microcystins are widespread throughout a number of California water bodies (unpublished data). The widespread detection of cyanobacterial toxins in California waters led the State of California to develop more proactive monitoring and alert efforts through the establishment of the California Cyanobacteria Harmful Algal Bloom (CCHAB) Network in 2013. One immediate recommendation from the CCHAB Network has been to explore the use of airborne or satellite remote sensing for detection of potentially harmful cyanobacterial blooms in State waters.

Remote sensing has been used successfully in many other freshwater systems, but often relies on algorithms designed for a specific sensor (e.g. Hunter, Tyler, Carvalho, Codd, & Maberly, 2008, 2010, Hunter, Tyler, Willby, & Glivear, 2008; Kutser, 2009; Simis et al., 2005; Vincent et al., 2004). Wynne et al. (2008, 2010) describe one of the most successful operational applications of remote sensing data for tracking CyanoHAB events. This system utilizes the CI derived from MERIS imagery to predict the onset and transport of blooms in the Laurentian Great Lakes. One aspect of their approach is utilization of spectral shape algorithms to reduce sensitivity to atmospheric correction issues. MERIS has also proven useful in other small inland lakes (e.g. Matthews & Bernard, 2013) using similar spectral shape approaches. Unfortunately, the loss of MERIS precludes ongoing use of these data, and while MERIS Full Resolution (FR) provides global 300 m (nadir) resolution, this is still marginal for small water bodies such as Pinto Lake and Kelly Lake, which would be covered by just 4 pixels integrating signals from both land and water. This limitation led us to examine other opportunistic datasets that could be used to identify potential cyanobacterial blooms.

4.1. Development of novel indices

MASTER is frequently flown in California, and was flown as part of both the NASA SARP program and the HyspIRI Airborne Campaign. Given the frequent availability of free imagery and the high spatial resolution, this sensor could provide a valuable record for mapping the occurrence of CyanoHABs in California waters. However, MASTER is missing the 681 nm band used for the CI algorithm, and generally is not optimized for water retrievals. Despite these limitations, we show

that alternative algorithms can be developed that work with MASTER, potentially expanding the application of spectral shape algorithms to other airborne and satellite sensors that were previously discounted because of non-optimal wavelengths for CI and similar algorithms.

Microcystis and other surface bloom-forming cyanobacteria such as *Anabaena* and *Aphanizomenon* exhibit relatively high backscattering ratios compared to other living cells due to their small size, presence of vacuoles, and for the latter two, presence of heterocysts (specialized cells used for nitrogen fixation) and akinetes (specialized resting-stage cells). The gas vesicles in *Microcystis* also alter its scattering phase function compared to *Microcystis* cells with collapsed gas vesicles and other non-vesicle bearing cyanobacteria genera. Specifically, scattering at forward angles is decreased while scattering at backward angles is increased (Volten et al., 1998). Thus, it is anticipated that the backscatter ratio for *Microcystis* is higher than for other cyanobacteria. This suggests that an algorithm based on the scattering properties of cyanobacteria may be an effective alternative to the large class of algorithms taking advantage of phycocyanin absorption. This led to SLH. While this is clearly a limited dataset, the potential use of SLH shows significant promise (Figs. 6, 7), and does as well or better than CI for Pinto Lake.

A significant shortcoming of existing cyanobacterial algorithms is that most fail to discriminate between cyanobacteria genera (Kutser, 2009). Numerous cyanobacteria are capable of producing blooms, and may or may not possess the capability to produce a variety of toxic compounds (c.f. O'Neil et al., 2012). AMI takes advantage of the optical differences between *Aphanizomenon* and *Microcystis* to provide a mechanism for classifying cyanobacteria into three clusters; strongly dominated by *Aphanizomenon*, strongly dominated by *Microcystis*, and mixed assemblages. Since only *Microcystis* produces microcystins in California water bodies, this provides additional information about the probability of toxins as a function of bloom type.

Application of the AMI algorithm is ideally implemented on pixels previously identified using either the CI or SLH algorithms as potential cyanobacterial blooms. The lack of empirical data for other bloom-forming cyanobacteria such as *Anabaena* and *Planktothrix* is also a potential limitation that would need to be addressed before this approach was implemented in other water bodies. Another potential failure of AMI as a predictor of toxic blooms is that extended presence of a "mixed" bloom such as occurred in 2013 is difficult to interpret. We note that this mixed bloom was still associated with toxin, albeit at lower duration and concentration than 2010–2012. Given the regular appearance of *Aphanizomenon* prior to *Microcystis*, followed by the (sometimes lengthy) period of mixed assemblages, separation of these genera optically may provide the potential to develop an early warning capability, with the caveat that the temporal separation between *Aphanizomenon* and *Microcystis* is variable, and sometimes quite short, while mixed assemblages may still contain toxic cells.

Using only the CI, several time periods from this study would be flagged as potentially dangerous blooms but exhibit low toxin levels (Fig. 7). These false positives could potentially be discriminated using AMI, which indicates that these events were not dominated by *Microcystis*. In contrast, increasing toxin concentrations were generally associated with dominance by *Microcystis* or mixed communities (lower AMI), regardless of the CI or SLH value. False negatives, where the indices suggest lack of CyanoHABs, are indicated by low or zero CI or SLH but high microcystin concentrations (Fig. 7). The same data plotted as AMI indicate that most of the points have some proportion of *Microcystis* (AMI < 5) indicative of the potential for toxin to be present. An issue would be that in a two-step process, failure to identify a bloom using CI or SLH would preclude application of AMI. While the relationships are somewhat noisy, the added information from AMI would be useful for semi-operational or operational use of imagery for prioritizing water bodies for more careful evaluation using the dual criteria of potential blooms present (CI and SLH) and then potential presence of *Microcystis* (AMI). The relative insensitivity of these indices, which rely on spectral shape, to noisy data and poor atmospheric correction suggest that routine application to imagery collected opportunistically or from future satellite sensors could be conducted with minimal cost and effort.

4.2. Future applications

Cyanobacterial blooms are increasingly prevalent worldwide (O'Neil et al., 2012; Paerl & Huisman, 2008, 2009). The tendency of these cyanobacterial blooms to be surface-intensified clearly suggests that remote sensing can provide a significant benefit in monitoring and forecasting these events. In California, there is increasing concern with the frequency and widespread prevalence of toxins in multiple watersheds (Butler et al., 2009, 2012) as well as increasing concern about the apparent trends in known hotspots such as the San Francisco Bay and Delta (Lehman et al., 2013). With a few exceptions, the more than 3000 named lakes and reservoirs in California are small, similar in size to Pinto Lake and Kelly Lake, and are in remote or poorly monitored locations. Opportunistic data collections such as SARP and the HyspIRI Airborne Campaign provide an opportunity to collect data at appropriately high spatial resolution over large swaths of California. These data also provide excellent proxies for future satellite missions such as OLCI, to be launched on Sentinel-3 by the European Space Agency, the HyspIRI, and the Pre-Aerosol Clouds and Ocean Ecosystem (PACE) sensors to be launched by NASA.

Since CI, SLH, and AMI require a small subset of bands (Fig. 2, Table 3), spectral requirements for application of these algorithms are minimal. The demonstrated insensitivity to poor atmospheric correction suggest that beyond MASTER, other commonly available airborne platforms such as the Advanced Visible/Infrared Imaging Spectrometer (AVIRIS), Next Generation AVIRIS (AVIRISng; Hamlin et al., 2011), and the Portable Remote Imaging Spectrometer (PRISM; Mouroulis et al., 2012) would all be suitable with very little additional processing, increasing the ability to use opportunistic data collections from both airborne and satellite platforms.

The imagery (Fig. 1 inset) from AVIRIS for Pinto Lake provides an example of what HyspIRI would provide at 60 m resolution. The expected return rate for HyspIRI of 19 days (Devred et al., 2013) limits applicability, particularly when non-optimal days (e.g. clouds, fog) are factored in. While the return rate is not ideal for tracking blooms, the bloom "season" typically lasts many weeks to months in Pinto Lake (Fig. 3). HyspIRI imagery could be combined with other opportunistic imagery from airborne, satellite, or International Space Station platforms to increase resolution. Taking advantage of other sensors such as PACE and OLCI would also refine the temporal resolution. Both the CI and SLH require a small subset of bands (Table 3). OLCI has the same bands as MERIS so CI is directly applicable; OLCI also has comparable bands for SLH (655, 709, 754 nm, versus 654,

714, 754 nm for MASTER). The AMI should be applicable to PACE given the planned spectral range and resolution (350–800 nm, ~5 nm resolution), which is comparable to HICO (400–900 nm, ~5.7 nm resolution). OLCI also has bands that could approximate AMI (510, 560, 620, 665 nm) but the lack of a ~650 nm band could be problematic. With either OLCI or PACE, imagery would be limited to large lakes and reservoirs where the ground sampling resolution is sufficient for tracking those water bodies, since OLCI and PACE will have 260 × 300 m and 1000 m (at nadir) respectively, with a possibility of increased, but still less than optimal, spatial resolution (300 m) for PACE depending on the final configuration of the sensor. In California, these lakes and reservoirs would include large water bodies such as Clear Lake, Lake Shasta, Lake Elsinore, and the Salton Sea.

5. Conclusions

Refinements to existing remote sensing spectral shape methods relying on phycocyanin absorption and scattering of cyanobacteria show promise for application to small inland water bodies. The potential to separate genera greatly enhances the utility of these methods for watersheds where there is clear differentiation in toxigenic status, such as the occurrence of non-toxic *Aphanizomenon* and toxic *Microcystis* in central California. While the data used as part of this analysis are limited in geographical scope and number of validation measurements, the successful application to HICO with minimal processing (including no optimization of the atmospheric correction) is encouraging. As new sensors come online in the next few years these methods have the potential to quickly and easily identify potentially impacted lakes and water bodies, thus greatly improving our ability to monitor, manage, and mitigate the growing threat of cyanobacterial harmful algal blooms.

References

Backer, L. C., McNeel, S. V., Barber, T., Kirkpatrick, B., Williams, C., Irvin, M., et al. (2010). Recreational exposure to microcystins during algal blooms in two California lakes. *Toxicon, 55*, 909–921.

Baxa, D. V., Kurobe, T., Ger, K. A., Lehman, P. W., & The, S. J. (2010). Estimating the abundance of toxic *Microcystis* in the San Francisco Estuary using quantitative Q-PCR. *Harmful Algal Blooms, 9*, 342–349.

Butler, N., Carlisle, J., & Linville, R. (2012). *Toxicological summary and suggested action levels to reduce potential adverse health effects of six cyanotoxins.* Integrated Risk Assessment Branch, Office Environmental Health and Hazard Assessment, California Environmental Protection Agency (26 pp.).

Butler, N., Carlisle, J. C., Linville, R., & Washburn, B. (2009). *Microcystins: A brief overview of their toxicity, and effects, with special reference to fish, wildlife, and livestock.* Integrated Risk Assessment Branch, Office Environmental Health and Hazard Assessment, California Environmental Protection Agency (17 pp.).

Carmichael, W. W. (2001). Health effects of toxin-producing cyanobacteria: "The CyanoHABs". *Human and Ecological Risk Assessment International Journal, 7*, 1393–1407.

Davis, T. W., Berry, D. L., Boyer, G. L., & Gobler, C. J. (2009). The effects of temperature and nutrients on the growth dynamics of toxic and non-toxic strains of *Microcystis* during cyanobacterial blooms. *Harmful Algae, 8*, 715–725.

Devred, E., Turpie, K. R., Moses, W., Klemas, V. V., Moisan, T., Babin, M., et al. (2013). Future retrievals of water column bio-optical properties using the hyperspectral infrared imager (HyspIRI). *Remote Sensing, 5,* 6812–6837.

Fetcho, K. (2007). *Klamath river blue-green algae summary report.*

Gao, B. -C., Montes, M. J., Ahmad, Z., & Davis, C. O. (2000). Atmospheric correction algorithm for hyperspectral remote sensing of ocean color from space. *Applied Optics, 39*(6), 887–896.

Gibble, C. M., & Kudela, R. M. (2014). Detection of persistent microcystin toxins at the land-sea interface in Monterey Bay, California. *Harmful Algae, 39,* 146–153.

Gilroy, D. J., Kauffman, K. W., & Hall, R. A. X. H. S. C. F. (2000). Assessing potential health risks from microcystin toxins in blue-green algae dietary supplements. *Environmental Health Perspectives, 108,* 435–439.

Gower, J. F., Doerffer, R. R., & Borstad, G. A. (1999). Interpretation of the 685 nm peak in water-leaving radiance spectra in terms of fluorescence, absorption and scattering, and its observation by MERIS. *International Journal of Remote Sensing, 20,* 1771–1786.

Guo, L. (2007). Ecology: Doing battle with the green monster of Taihu Lake. *Science, 317,* 1166.

Hamlin, L., Green, R. O., Mouroulis, P., Eastwood, M., Wilson, D., Dudik, M., et al. (2011). Imaging spectrometer science measurements for terrestrial ecology: AVIRIS and new developments. *Aerospace Conference, 2011 IEEE* (pp. 1–7).

Hook, S. J., Myers, J. J., Thome, K. J., Fitzgerald, M., & Kahle, A. B. (2001). The MODIS/ASTER airborne simulator (MASTER)—A new instrument for earth science studies. *Remote Sensing of Environment, 76,* 93–102.

Hunter, P. D., Tyler, A. N., Carvalho, L., Codd, G. A., & Maberly, S. C. (2010). Hyperspectral remote sensing of cyanobacterial pigments as indicators for cell populations and toxins in eutrophic lakes. *Remote Sensing of Environment, 114,* 2705–2718.

Hunter, P. D., Tyler, A. N., Willby, N. J., & Glivear, D. J. (2008). The spatial dynamics of vertical migration by *Microcystis* aeruginosa in a eutrophic shallow lake: A case study using high spatial resolution time-series airborne remote sensing. *Limnology and Oceanography, 53,* 239102406.

IOCCG (2014). Ocean Land Colour Instrument onboard Sentinel-3 (ESA). http://www.ioccg.org/sensors/olci.html (accessed 3 October 2014)

Jacoby, J. M., Collier, D. C., Welch, E. B., Hardy, F. J., & Crayton, M. (2000). Environmental factors associated with a toxic bloom of *Microcystis aeruginosa. Canadian Journal of Fisheries and Aquatic Sciences, 57,* 231–240.

Johnston, B. R., & Jacoby, J. M. (2003). Cyanobacterial toxicity and migration in a mesotrophic lake in western Washington, USA. *Hydrobiologia, 495,* 79–91.

Kahru, M. (1997). Using satellites to monitor large-scale environmental change in the Baltic Sea. In M. Kahru, & C. W. Brown (Eds.), *Monitoring algal blooms: New techniques for detecting large-scale environmental change* (pp. 43–61). Springer- Verlag.

Kudela, R. M. (2011). Characterization and deployment of solid phase adsorption toxin tracking (SPATT) resin for monitoring of microcystins in fresh and saltwater. *Harmful Algae*(11), 117–125.

Kudela, R. M., Garfield, N., & Bruland, K. W. (2006). Bio-optical signatures and biogeochemistry from intense upwelling and relaxation in coastal California. *Deep Sea Research, Part II, 53,* 2999–3022.

Kurobe, T., Baxa, D. V., Mioni, C. E., Kudela, R. M., Smythe, T. R., Waller, S., et al. (2013). Identification of harmful cyanobacteria in the Sacramento-San Joaquin Delta and Clear Lake, California by DNA barcoding. *SpringerPlus, 2,* 491. http://dx.doi.org/10.1186/2193-1801-2-491.

Kutser, T. (2009). Passive optical remote sensing of cyanobacteria and other intense phytoplankton blooms in coastal and inland waters. *International Journal of Remote Sensing, 30,* 4401–4425.

Lee, Z. P., Carder, K. L., Steward, R. G., Peacock, T. G., Davis, C. O., & Mueller, J. L. (1997). Remote sensing reflectance and inherent optical properties of oceanic waters derived from above-water measurements. *Proceedings of SPIE 2963, Ocean Optics XIII, 160.*

Lehman, P. W., Boyer, G., Hall, C., Waller, S., & Gerhrts, K. (2005). Distribution and toxicity of a new colonial *Microcystis aeruginosa* bloom in the San Francisco Bay Estuary, California. *Hydrobiologia, 541,* 87–99.

Lehman, P. W., Boyer, G., Satchwell, M., & Waller, S. (2008). The influence of environmental conditions on the seasonal variation of *Microcystis* cell density and microcystins concentration in San Francisco Estuary. *Hydrobiologia, 600,* 187–204.

Lehman, P. W., Marr, K., Boyer, G. L., Acuna, S., & Teh, S. J. (2013). Long-term trends and causal factors associated with *Microcystis* abundance and toxicity in San Francisco Estuary and implications for climate change impacts. *Hydrobiologia, 718,* 141–158.

Lehman, E. M., McDonald, K. E., & Lehman, J. T. (2009). Whole lake selective withdrawal experiment to control harmful cyanobacteria in an urban impoundment. *Water Research, 43,* 1187–1198.

Lucke, R. L., Corson, M., McGlothlin, N. R., Butcher, S. D., & Wood, D. L. (2010, August). The hyperspectral imager for the coastal ocean (HICO): Fast build for the ISS. *SPIE optical engineering + applications. International Society for Optics and Photonics* (pp. 78130D-78130D).

Matthews, M. W., & Bernard, S. (2013). Characterizing the absorption properties for remote sensing of three small optically-diverse South African reservoirs. *Remote Sensing, 5,* 4370–4404.

Matthews, M. W., Bernard, S., & Robertson, L. (2012). A new algorithm for detecting trophic status (chlorophyll-a), cyanobacterial-dominanance, surface scums and floating vegetation in coastal and inland waters from MERIS. *Remote Sensing of Environment, 124,* 637–652.

McDonald, K. E., & Lehman, J. T. (2013). Dynamics of *Aphanizomenon* and *MIcrocystis* (cyanobacteria) during experimental manipulation of an urban impoundment. *Lake and Reservoir Management, 29,* 103–115.

Miller, M. A., Kudela, R. M., & Jessup, D. A. (2012). When marine ecosystems fall ill. *The wildlife professional, spring 2012* (pp. 44–48).

Miller, M. A., Kudela, R. M., Mekebri, A., Crane, D., Oates, S. C., Tinker, M. T., et al. (2010). Evidence for a novel marine harmful algal bloom: Cyanotoxin (microcystin) transfer from land to sea otters. *PLoS ONE, 5,* e12576.

Mobley, C. D. (1995). *Light and water: Radiative transfer in natural waters.* San Diego, CA: Academic Press (592 pp.).

Moisander, P. H., Lehman, P. W., Ochiai, M., & Corum, S. (2009). Diversity of the toxic cyanobacterium *Microcystis aeruginosa* in the Klamath River and San Francisco Bay delta, California. *Aquatic Microbial Ecology, 57,* 19–31.

Morel, A. (1998). Optical modeling of the upper ocean in relation to its biogenous matter content (case I waters). *Journal of Geophysical Research, 93,* 10749–10768.

Mouroulis, P., Van Gorp, B., Green, R. O., Eastwood, M., Boardman, J., Richardson, B. S., et al. (2012). Portable remote imaging spectrometer (PRISM): Laboratory and field calibration. *SPIE optical engineering + applications. International society for optics and photonics* (pp. 85150F-85150F).

O'Neil, J. M., Davis, T. W., Burford, M. A., & Gobler, C. J. (2012). The rise of harmful cyanobacteria blooms: The potential roles of eutrophication and climate change. *Harmful Algae, 14,* 313–334.

Ogashawara, I., Misra, D. R., Mishra, S., Curtarelli, M. P., & Stech, J. L. (2013). A performance review of reflectance based algorithms for predicting phycocyanin concentrations in inland waters. *Remote Sensing, 5,* 4774–4798.

PACE (2012). Pre-Aerosol, Clouds, and ocean Ecosystem (PACE) Mission Science Definition Team Report. Available at http://decadal.gsfc.nasa.gov/pace_documentation/PACE_SDT_Report_final.pdf

Paerl, H. W. (2008). Nutrient and other environmental controls of harmful cyanobacterial blooms along the freshwater–marine continuum. In K. H. Hudnell (Ed.), *Cyanobacterial harmful algal blooms: State of the science and research needs advances in experimental medicine and biology. 619.* (pp. 217–237). New York: Springer Science + Business Media.

Paerl, H. W., Hall, N. S., & Calandrino, E. S. (2011). Controlling harmful cyanobacterial blooms in a world experiencing anthropogenic and climatic-induced change. *Science of the Total Environment, 409,* 1739–1745.

Paerl, H. W., & Huisman, J. (2008). Climate: Blooms like it hot. *Science, 320,* 57–58.

Paerl, H. W., & Huisman, J. (2009). Climate change: A catalyst for global expansion of harmful cyanobacterial blooms. *Environmental Microbiology Reports, 1,* 27–37.

Paerl, H. W., & Otten, T. G. (2013). Harmful cyanobacterial blooms: Causes, consequences, and controls. *Microbial Ecology, 65,* 995–1010.

Ryan, J. P., Davis, C. O., Tufillaro, N. B., Kudela, R. M., & Gao, B. -C. (2014). Application of the hyperspectral imager for the coastal ocean to phytoplankton ecology studies in Monterey Bay, CA, USA. *Remote Sensing, 6,* 1007–1025.

Sampath-Wiley, P., & Neefus, C. D. (2007). An improved method for estimating R-phycoerythrin and R-phycocyanin contents from crude aqueous extracts of *Porphyra* (Banglales, Rhodophyta). *Journal of Applied Phycology, 19,* 123–129.

Sellner, K. G. (1997). Physiology, ecology, and toxic properties of marine cyanobacteria blooms. *Limnology and Oceanography, 42,* 1089–1104.

Simis, S. G. H., Peters, S. W. M., & Gons, H. J. (2005). Remote sensing of the cyanobacteria pigment phycocyanin in turbid inland water. *Limnology and Oceanography, 50,* 237–245.

Simis, S. G. H., Ruiz-Verdu, A., Dominguez, J. A., Pena-Martinez, R., Peters, S. W. M., & Gons, H. J. (2007). Influence of phytoplankton pigment composition on remote sensing of cyanobacterial biomass. *Remote Sensing of Environment, 106,* 414–427. http://dx.doi.org/10.1016/j.rse.2006.09.008.

Tsuji, K., Nalto, S., Kondo, F., Ishikawa, N., Watanabe, M. F., Suzuki, M., et al. (1994). Stability of microcystins from cyanobacteria: Effect of light on decomposition and isomerization. *Environmental Science and Technology, 1094*(28), 173–177.

Vincent, R. K., Quin, X., McKay, R. M. L., Miner, J., Czajkowski, K., Savino, J., et al. (2004). Phycocyanin detection from LANDSAT TM data for mapping cyanobacterial blooms in Lake Erie. *Remote Sensing of Environment, 89,* 381–392. http://dx.doi.org/10.1016/j.rse.2003.10.014.

Volten, H., de Haan, J. F., Hovenier, J. W., Schreurs, R., Vassen, W., Dekker, A. G., et al. (1998). Laboratory measurements of angular distributions of light scattered by phytoplankton and silt. *Limnology and Oceanography, 43,* 1180–1197.

Welker, M., & Steinburg, C. (2000). Rates of humic substance photosensitized degradation of microcystin-LR in natural waters. *Environmental Science and Technology, 34,* 3415–3419.

Wynne, T. T., Stumpf, R. P., Tomlinson, M. C., & Dyble, J. (2010). Characterizing a cyanobacterial bloom in western Lake Erie using satellite imagery and meteorological data. *Limnology and Oceanography, 55,* 2025–2036.

Wynne, T. T., Stumpf, R. P., Tomlinson, M. C., Warner, R. A., Tester, P. A., Dyble, J., et al. (2008). Relating spectral shape to cyanobacterial blooms in the Laurentian Great Lakes. *International Journal of Remote Sensing, 29,* 3665–3672. http://dx.doi.org/10.1080/01431160802007640.

Zehnder, A., & Gorham, P. R. (1960). Factors influencing the growth of *Microcystis aeruginosa. Canadian Journal of Microbiology, 6,* 645–660.